https://doi.org/10.5194/gmd-2021-410
Preprint. Discussion started: 14 January 2022

Geoscientific Model Development Discussions

The Impact of Hurricane Disturbances on a Tropical Forest: Implementing a Palm Plant Functional Type and Hurricane Disturbance Module in ED2-HuDi V1.0

Jiaying Zhang[1], Rafael L. Bras[1], Marcos Longo[2,3], Tamara Heartsill Scalley[4]

[1]School of Civil and Environmental Engineering, Georgia Institute of Technology, Atlanta, GA, United States
[2]Jet Propulsion Laboratory, California Institute of Technology, Pasadena, CA, United States
[3]Climate and Ecosystem Sciences Division, Lawrence Berkeley National Laboratory, Berkeley, CA, United States
[4]USDA Forest Service, International Institute of Tropical Forestry, Río Piedras, PR, United States.

Correspondence to: Jiaying Zhang (jiaying.zhang@gatech.edu); Rafael L. Bras (rlbras@gatech.edu)

https://doi.org/10.5194/gmd-2021-410
Preprint. Discussion started: 14 January 2022

Geoscientific Model Development Discussions

Abstract

Hurricanes commonly disturb and damage tropical forests. It is predicted that changes in climate will result in changes in hurricane frequency and intensity. Modeling is needed to investigate the potential response of forests to future disturbances. Unfortunately, existing models of forests dynamics are not presently able to account for hurricane disturbances. We implement the Hurricane Disturbance in the Ecosystem Demography model (ED2) (ED2-HuDi). The hurricane disturbance includes hurricane-induced immediate mortality and subsequent recovery modules. The parameterizations are based on observations at the Bisley Experimental Watersheds (BEW) in the Luquillo Experimental Forest in Puerto Rico. We add one new plant functional type (PFT) to the model—Palm, as palms cannot be categorized into one of the current existing PFTs and are known to be an abundant component of tropical forests worldwide. The model is calibrated with observations at BEW using the generalized likelihood uncertainty estimates (GLUE) approach. The optimal simulation obtained from GLUE has a mean relative error of -21%, -12%, and -15% for stem density, basal area, and aboveground biomass, respectively. The optimal simulation also agrees well with the observation in terms of PFT composition (+1%, -8%, -2%, and +9% differences in the percentages of Early, Mid, Late, and Palm PFTs, respectively) and size structure of the forest (+0.8% differences in the percentage of large stems). Lastly, using the optimal parameter set, we study the impact of forest initial condition on the recovery of the forest from a single hurricane disturbance. The results indicate that, compared to a no-hurricane scenario, a single hurricane disturbance has little impact on forest structure (+1% change in the percentage of large stems) and composition (< 1% change in the percentage of each of the four PFTs) but leads to 5% higher aboveground biomass after 80 years of succession. The assumption of a less severe hurricane disturbance leads to a 4% increase in aboveground biomass.

1 Introduction

Hurricanes are an important disturbance agent in tropical forests. They damage individual trees and reduce aboveground biomass (Zimmerman et al. 1994; Uriarte et al. 2019; Rutledge et al. 2021; Leitold et al. 2021; Zhang et al. in revision). In the long term, they alter forest species composition and structure (Royo et al. 2011; Heartsill Scalley 2017; Zhang et al. in revision).

Hurricane-induced mortality varies with many factors, including hurricane severity (Parker et al. 2018), environmental conditions (Uriarte et al. 2019; Hall et al. 2020), forest structure (Zhang et al. in revision), and traits and size of individual trees (Curran et al. 2008; Lewis and Bannar-Martin 2011). Trees with a larger diameter have been found to be more resistant to wind forces but more likely to suffer broken branches (Lewis and Bannar-Martin 2011). Species with higher wood density tend to suffer less from hurricane disturbances (Zimmerman et al. 1994; Curran et al. 2008). Hurricanes with heavier rainfall and stronger wind generally lead to higher mortality (Uriarte et al. 2019; Hall et al. 2020). However, forests with a more wind-resistant structure and composition experience lower mortality even during a stronger hurricane event (Zhang et al. in revision).

The recovery from hurricanes also depends on many factors, such as the disturbance severity (Walker 1991; Everham and Brokaw 1996; Cole et al. 2014; Heartsill Scalley 2017) and traits of individual species (Curran et al. 2008; Lewis and Bannar-Martin 2011). Species with lower wood density have a faster resprouting (Paz et al. 2018)

https://doi.org/10.5194/gmd-2021-410
Preprint. Discussion started: 14 January 2022


Geoscientific Model Development Discussions

and biomass recovery (Curran et al. 2008). The resprouting of some species further varies with time since disturbance (Brokaw 1998; Zhang et al. in revision). Less severe disturbances lead to a faster recovery and a higher recovery equilibrium (Wang and Eltahir 2000; Parker et al. 2018). For example, observations on a tropical forest canopy in western Mexico after two hurricanes—category 2 Jova and category 4 Patricia—showed that hurricane Jova destroyed 11% of the aboveground biomass while hurricane Patricia destroyed 23%; the recovery was more rapid after the less intense hurricane Jova (Parker et al. 2018). Wang and Eltahir (2000) provided theoretical and numerical analyses on multiple-equilibrium nature of a regional climate system. Their results showed that the recovery speed and the equilibrium state of the coupled biosphere-atmosphere system are sensitive to the initial vegetation condition impacted by disturbances.

In the past decades, there has been a strong effort to incorporate functional diversity in terrestrial biosphere models (Moorcroft et al. 2001; Sakschewski et al. 2016; Fisher et al. 2018; Fisher and Koven 2020). This effort acknowledges the variability in traits and trade-offs that exist in tropical forests (e.g., Baraloto et al. 2010). Fast growing pioneer species have low wood density, establish and recruit in open gaps formed after disturbances and grow rapidly in the high light environment. They dominate the early successional stage of the recovery, and thus are categorized as Early plant functional type (PFT). Species that have intermediate growth and are somewhat shade tolerant dominate the plant community in the mid successional stage after a disturbance, and thus are categorized as Mid PFT. Species that have slow growth and are shade tolerant dominate a plant community in the late successional stage after a disturbance, and thus are categorized as Late PFT. One important and distinct species in tropical forests in the Caribbean islands is the palm species *Prestoea montana*. The palm species is more resistant to hurricane damage compared to trees (Francis and Gillespie 1993). Moreover, the palm species cannot be classified into one of the successional PFTs, because palms possess some early successional traits, such as low "wood" density and high fecundity under open canopy (Lugo and Rivera Batlle 1987; Lugo et al. 1998), that allow them to recruit quickly when the canopy opens (Zhang et al. in revision); and some late successional traits, such as tolerance to shade (Ma et al. 2015), that allow them to thrive when the canopy closes (Zhang et al. in revision). To account for these unique characteristics, we define a Palm PFT.

In this paper, we describe the implementation of hurricane mortality and recovery modules that account for the variation with disturbance severity, forest resistance state, PFT and diameter size of individual stems in the Ecosystem Demography model (ED2). The model is then used to study the recovery of a tropical rainforest after hurricane disturbances. The results indicate that a single hurricane disturbance has little impact on forest structure and composition but enhances the aboveground biomass accumulation of a tropical rainforest.

2 Methods and Materials

2.1 Model Description

The Ecosystem Demography model (ED) is a cohort-based model, and it describes the growth, reproduction, and mortality of each cohort in each patch in a forest site. A cohort is a group of stems with the same PFT and similar diameter size and age. A patch is an area with the same environmental condition and disturbance history. The model

https://doi.org/10.5194/gmd-2021-410
Preprint. Discussion started: 14 January 2022


Geoscientific Model Development Discussions

simulates transient fluxes of carbon, water, and energy during short-term physiological responses and long-term ecosystem composition and structure responses to changes in environmental conditions. The second version of the ED model, ED2, modifies the calculations of radiation and evapotranspiration of the original ED model, leading to a more realistic long-term response of ecosystem composition and structure to atmospheric forcing (Medvigy et al. 2009; Longo et al. 2019b). Details of the ED and ED2 models can be found in Moorcroft et al. (2001), Medvigy et al. (2009), and Longo et al. (2019a). Here we add a new PFT (Palm) and implement hurricane disturbance in the ED2 model, and we name it ED2-HuDi V1.0.

2.1.1 Adding Palm as a New PFT

The standard ED2 model represents a variety of broadleaf trees, needleleaf trees, grasses and lianas (Albani et al. 2006; Medvidy et al. 2009; Longo et al. 2019a; di Porcia e Brugnera et al. 2019). Yet, to date, none of the existing PFTs describe the traits of palms, even though palms are a globally abundant component of tropical forests (Muscarella et al. 2020). Since there is little knowledge about the traits of Palm. We do know that palms have low "wood density" of ~0.25 g cm^{-3} (Zanne et al. 2009; Chave et al. 2009) and grow fast in open canopies like early tropical trees and are tolerant to shade like late tropical trees (Zhang et al. in revision). Hence, we assume that the traits of Palm have the same probability distributions as those of late tropical trees except for wood density which is assumed the same as that of early tropical trees.

2.1.2 Modifying the Allometric Relationship

The H-DBH allometric relationships for four tropical PFTs (Early, Mid, Late, and Palm) come from census data at Bisley Experimental Watersheds (BEW) in the Luquillo Experimental Forest in Puerto Rico. The relationships take the form,

$$H = a\, DBH^{b}\,, \tag{1}$$

where a and b are PFT-specific scale and shape parameters (Zhang et al. in revision). The diameter range for the Palm PFT is between 10 and 20 cm while that for the tree PFTs is between 2.5 and 90 cm. The scale parameter a is 1.6388, 2.2054, 2.3833, and 0.1628 for Early, Mid, Late, and Palm PFT, respectively. The shape parameter b for the four PFTs are 0.80, 0.64, 0.59, and 1.47 (Table S1). Palm has a smaller scale parameter and a significantly larger shape parameter, demonstrating that palms are shorter than other PFTs given the same DBH. The constrained diameter range and the H-DBH allometry of Palm makes it difficult for palms to access sunlight and would normally prevent them from establishing in the ED2 model. A previous study implementing liana to the ED2 model also experienced similar issues. They then were to use an allometry for liana with DBH between 3 and 20 cm and the allometry of early successional trees for lianas with DBH less than 3 cm (di Porcia e Brugnera et al. 2019). Following a similar approach and to make sure Palm has reasonable opportunity to compete with a reasonable diameter range, we assume that the minimum height of Palm in the model is 4.8 m (corresponding to 10 cm DBH of Palm; other PFTs have a minimum height of 1.5 m for recruitment), and when Palm grows to a height of 18 m (corresponding to 20 cm DBH), they will allocate all the carbon to reproduction instead of growth (relative allocation to reproduction is 1 for Palm, and 0.3 for other PFTs) (Table S1).

https://doi.org/10.5194/gmd-2021-410
Preprint. Discussion started: 14 January 2022

Geoscientific Model Development Discussions

115 For other allometric relationships, such as leaf biomass-DBH, structural biomass-DBH, and crown area-DBH
116 relationships, we used the model default for Early, Mid, and Late PFTs, and assumed that Palm has the same
117 relationships as Early (Figure S1).

118 **2.1.3 Implementing Hurricane Disturbance**

119 The ED2 model accounts for several types of disturbances, such as fires, land use, logging (Albani et al. 2006; Longo
120 et al. 2019a), but not hurricane disturbance. To account for hurricane impacts, we implement a hurricane-induced
121 wind mortality module and a seedling recovery module in the model. The wind mortality module consists of two
122 parts—the disturbance rate of the forest area (λ_d) and the survivorship of each cohort ($\boldsymbol{s}_c$) in the disturbed areas. The
123 disturbance rate (λ_d) is the ratio of the area disturbed to the total area of the forest and it is a constant across patches.
124 The survivorship of each cohort ($\boldsymbol{s}_c$) is the ratio of the cohort density that survived to the cohort density before the
125 disturbance, and it is cohort dependent. The cohorts that survived in disturbed areas will make up a new patch with
126 area equal to the disturbed area. In this study, we assume that the forest is fully disturbed and $\lambda_d = 1$. The survivorship
127 of each cohort $\boldsymbol{s}_c$ is calculated as $\boldsymbol{s}_c = 1 - \boldsymbol{\lambda}_c$, where $\boldsymbol{\lambda}_c$ is the mortality of each cohort. Based on previous analyses, $\boldsymbol{\lambda}_c$
128 varies with hurricane strength, forest structure, the PFT category and the DBH size of the cohort (Zhang et al. in
129 revision). First, we implement a binary model for the mortality with respect to hurricane wind, where mortality occurs
130 when hurricane wind exceeds a threshold and no mortality otherwise. This binary model is built on the binary
131 relationship between hurricane-induced forest damage and hurricane wind speed from nine hurricane events at BEW
132 between 1989 and 2017 (Supplementary Information S1, S2, and S3). The wind speed threshold was set at 41 m s^{-1}
133 because the strongest hurricane wind that caused no damage to the forest at BEW was 40 m s^{-1} from hurricane Georges
134 in 1998 and the lowest wind speed that caused damage to the forest was 42 m s^{-1} from hurricane Maria in 2017
135 (Supplementary Information S1, S2, and S3). Given mortality, the rate of each cohort ($\boldsymbol{\lambda}_c$) is a continuous function of
136 the size structure of the forest, represented by the proportion of large stems (DBH ≥ 10 cm) to the total recruited stems
137 (DBH ≥ 2.5 cm). Figure 1 shows the mortality of each PFT and DBH class during two hurricane events (Hugo and
138 Maria) based on census observations at BEW (see Sect. 2.2). We fit a logistic function to the mortality-structure pair
139 of each PFT and DBH class based on the observed pairs of mortality and structure from the two hurricane events.

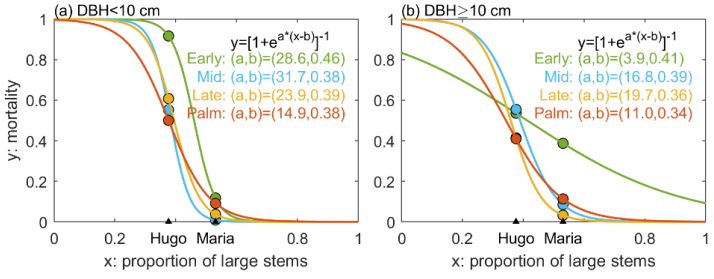

140

141 **Figure 1.** The mortality for each PFT and DBH class. The dots represent observed mortality and proportion of large stems pairs
142 from hurricane Hugo and hurricane Maria (Zhang et al. in revision). Four colors represent four PFTs. The solid lines represent the
143 estimated mortality as a logistic function of the proportion of large stems. The panel on the left is for small stems and that on the
144 right is for large stems.

145

https://doi.org/10.5194/gmd-2021-410
Preprint. Discussion started: 14 January 2022

Geoscientific Model Development Discussions

Hurricanes not only cause immediate stem mortality, but also affect the establishment of seedlings by opening the canopy (Brokaw 1998). Brokaw (1998) pointed out that hurricanes promote germination and seedling establishment of the early successional species *C. schreberiana*, and that the seedling establishment ends shortly after the disturbance as the canopy closes. The census data at BEW also show abundant recruitments of the Early PFT in the first 20 years after hurricane Hugo and decreasing recruitment with time (Zhang et al. in revision). Therefore, we implement a recovery module where the seedling density from seed rain (n_s; individuals m^{-2} yr^{-1}) decreases with time since the last disturbance, and the reduction varies with PFT categories as:

$$n_s = n_0 \exp(-\alpha t)\,, \quad (2)$$

where n_s is the seedling density t years after last hurricane disturbance, n_0 and α are PFT-dependent parameters. Specifically, Mid, Late, and Palm PFTs maintain a low but constant seedling density (n_0 = 0.05 individuals m^{-2} yr^{-1} and α = 0 yr^{-1}). The Early PFT has high seedling density (n_0 = 0.2 individuals m^{-2} yr^{-1}) shortly after a hurricane disturbance and the seedling rate decreases to the same value as other PFTs about 20 years after the disturbance (α = 0.06 yr^{-1}), and it continues to decrease thereafter (Figure 2).

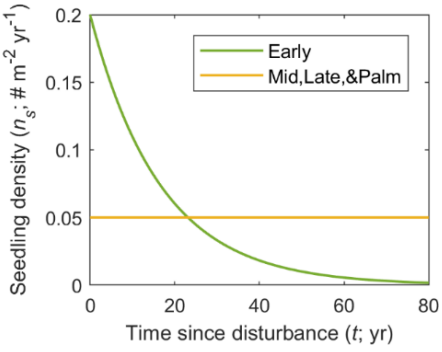

Figure 2. The seedling density for each PFT after a disturbance.

2.2 Census Observations

Tree censuses were carried out in BEW in the Luquillo Experimental Forest in Puerto Rico starting in 1989, three months before hurricane Hugo (pre-Hugo 1989), and repeated three months after hurricane Hugo (post-Hugo 1989), and then every five years since then (1994, 1999, 2004, 2009, 2014). The census recorded the diameter at breast height (DBH) and species of each stem with DBH ≥ 2.5 cm in 85 dynamics plots in the forest. The last census was conducted three months after hurricane Maria, and recorded auxiliary damage information of each stem. The detailed description of the study site and the census observations can be found in Zhang et al. (in review) and the census data between 1989 and 2014 are from Zhang et al. (in review) and the post-Maria census data are from (Zhang et al. 2020). Species are categorized into four PFTs: early, mid, late successional tropical trees, and palms (Early, Mid, Late, and Palm PFT, respectively) following Zhang et al. (in review). The stem density, DBH growth rate, and basal area are calculated from the census data for each PFT in each census, and the aboveground biomass is estimated from DBH using the

https://doi.org/10.5194/gmd-2021-410
Preprint. Discussion started: 14 January 2022


Geoscientific Model Development Discussions

allometric relationship from Scatena et al. (1993). The census observations will be used for initializating, calibrating, and validating model simulations.

2.3 Model Calibration and Validation

2.3.1 The GLUE approach

The concept of Generalized Likelihood Uncertainty Estimates (GLUE) (Binley and Beven 1991; Beven and Binley 1992; Mirzaei et al. 2015) has been widely used to calibrate parameters in complex hydrological models. The steps of GLUE include 1) generating a number of samples of the parameter set from a prior distribution of the parameters, 2) running the simulation for each parameter set, 3) choosing a likelihood function (or weight function) to calculate the weight of each simulation based on observations and the estimated outputs from the model simulation, and 4) selecting the optimal parameter set and estimating the posterior distribution of the parameters and the posterior distribution of the output variables. Here we use GLUE, for the first time, to calibrate the parameters in the ED2 model.

To obtain the prior distribution of parameters, we build on a previous parameter sensitivity analysis using the ED2 model for a nearby forest in Puerto Rico by Feng et al. (2018). They demonstrated that model simulations are sensitive to ten parameters, listed in Table 1, and provided the posterior mean and 95% confidence limits of the parameters calibrated from plant traits observations using the Predictive Ecosystem Analyzer (PEcAn; LeBauer et al. 2013). We select the same parameters and use the posterior distribution of those parameters from Feng et al. (2018) as the prior distribution for the GLUE in our study. We cannot just use their parameter distributions as final results because our implementation has a site-specific set of allometric equations, explicitly represents palms as a separate PFT and considers hurricane disturbances (Sect. 2.1). Feng et al. (2018) reported only the mean and the upper and lower 95% confidence limits of the parameters (not the entire distribution), we assume that the parameters have lognormal distributions. For the Palm PFT, we assume that it has the same distributions as Late, except that the woody tissue density of Palm has the same distribution as that of Early. The dark respiration factor from Feng et al. (2018) has a too wide range (Wang et al. 2013), and thus we restrict it to a uniform distribution between 0.005 and 0.0175 for each PFT. Consistent with Meunier et al. (in revision), we found that model results are also sensitive to the parameter clumping factor (Figure S2). Therefore, we add the parameter of clumping to the set being calibrated. Clumping factor is defined as the projected area of leaves per unit ground area and affects the transmission of radiation (Chen and Black 1992); it ranges from zero to one with zero representing clumped in a single point (0-area) and one representing uniformly distributed in the unit area. Because of tree crowns, branches, and subbranches, leaves of plant canopy are not uniformly distributed per unit area nor clumped at a single point. We assume that the clumping factor is the same for all PFTs and the distribution of clumping factor is uniform between 0.2 and 0.8.

We sample 10,000 realizations for the 41 parameters (10 parameters for each of the four PFTs and the one clumping parameter for all PFTs) using the Latin Hypercube Sampling method embedded in MATLAB (Stein 1987). We initialize the model with the pre-Hugo 1989 observations and run the model for 29 years, corresponding to 1989–2018. The first 25 years (1989–2014) are used to calibrate the model with observations and the last four years (2015–2018) for validation. We calculate the mean squared errors (*MSE*) of each realization (j, j=1, 2, …, 10,000) for the calibration period,

https://doi.org/10.5194/gmd-2021-410
Preprint. Discussion started: 14 January 2022

Geoscientific Model Development Discussions

$$MSE_j = \frac{1}{nm}\sum_{t=1}^{m}\sum_{i=1}^{n}\left(\frac{X_{i,t,j} - Y_{i,t}}{\frac{1}{m}\sum_{t=1}^{m} Y_{i,t}}\right)^2, \quad (3)$$

where $X_{i,t,j}$ represents the j^{th} model simulations for variable i at time t, and $Y_{i,t}$ represents observations for variable i at time t. The variables used to calculate *MSE* are stem density (individuals m^{-2}), average DBH growth rate (cm (5 yr)$^{-1}$), and basal area (BA) (cm^2 m^{-2}) for the four PFTs (n=12) (Figure 3). Times are the six census years (m=6) with observations before hurricane Maria: post-Hugo 1989, 1994, 1999, 2004, 2009, 2014. Because BA is directly calculated from the DBH of each cohort and weighted by the stem density of the cohort, the size structure (distribution of stem DBHs) of the forest is implicitly represented with the variables overall stem density and total BA. Moreover, the PFT composition is explicitly represented with the PFT-specific variables. Therefore, the *MSE* metric implicitly measures the performance of a realization in describing the observed time series of the forest's size structure and PFT composition.

We select the simulation with the smallest *MSE* as the optimal simulation and the corresponding parameter set as the optimal parameter set. To obtain the posterior distribution of parameters, we first calculate the weight (likelihood) of each realization following Binley and Beven (1991),

$$w_j = MSE_j^{-K}, \quad (4)$$

which is then rescaled to sum to one ($w_j / \sum_{j=1}^{N} w_j$), where K is the parameter that controls the weight of each realization. When K = 0, every simulation will have equal weights and when K = ∞, the single best simulation will have a rescaled weight of 1 while all others being zero. We select K such that the weighted standard deviations from simulations are within and overlap as much as possible with the standard deviations of observations, indicating that the parameters in those weighted simulations are reasonable given the uncertainty of the observations (Freer et al. 1996). The weighted standard deviation of variable X is calculated as

$$\sigma_X = \sqrt{\sum_{j=1}^{N} w_j \left(X_j - m_X\right)^2}, \quad (5)$$

where $m_X = \sum_{j=1}^{N} w_j X_j$ is the weighted mean of the simulated variable. We find that K=8 has the best performance on the posterior estimates of output variables stem density, aboveground biomass, basal area, proportion of each PFT, and proportion of large stems (Figure 4, Figure S3, and Figure S4). Lastly, the posterior empirical cumulative distribution function (CDF) of the parameters is obtained as

$$F(P \le p) = \sum_{j:P_j \le p} w_j . \quad (6)$$

The posterior empirical CDFs are then fit to lognormal distributions.

2.3.2 Non-Hurricane Mortality

The non-hurricane mortality of palm is not well represented in the model (Figure S5), as initially calibrated. The observed non-hurricane mortality is an overall mortality regardless of the cause of the death and is calculated from non-hurricane censuses; whereas the non-hurricane mortality in model simulations includes aging mortality, competition mortality, and disturbance mortality. We turned off all disturbances except for hurricane and treefall

https://doi.org/10.5194/gmd-2021-410
Preprint. Discussion started: 14 January 2022

Geoscientific Model Development Discussions

disturbance. The disturbance mortality includes the background exogenous mortality rate (0.014 year^{-1} for small stems), and treefall disturbance rate (0.0126 year^{-1} for small stems and 0.014 year^{-1} for large stems). Competition mortality is related to the negative carbon balance due to light and water limitation and varies with cohorts. Aging mortality is the reciprocal of the longevity of the cohort without any biotic and abiotic influences, and it is modeled as a constant for each PFT depending on the wood density of the PFT (ρ_{PFT}) relative to the wood density of the Late PFT (ρ_{Late}): $0.15 \times (1 - \rho_{PFT}/\rho_{LATE})$ (Moorcroft et al. 2001). Since Palm has a much lower "wood" density (~0.25 g cm^{-3}) than the Late PFT (model default 0.9 g cm^{-3}), the aging mortality of Palm is ~0.1 year^{-1}, or the longevity of palms would be equivalent to ~10 years. However, this is in contrast to the average age of the palm species in the Luquillo Experimental Forest, which was found to be 61.1 years and the oldest palms were more than 100 years old in 1982 (Lugo and Rivera Batlle 1987). This suggests that the aging mortality of Palm calculated from its woody tissue density is a drastic overestimation. Therefore, we assume that the aging mortality of Palm is independent of its woody tissue density and is 0 year^{-1}, same as that of Late.

With a lower mortality (decreasing aging mortality from ~0.1 to 0), the density of Palm increases continuously in the forest because of continuously recruiting seedlings, while the density of other PFTs and the AGB of all PFTs are less affected (Figure S6). A previous study showed that hurricane disturbance can result in an increase in seed production in the palm species (Gregory and Sabat 1996). Therefore, we calibrate the seedling recovery module of Palm that we implemented in Sect. 2.1.3. Specifically, we test several recovery seedling densities (Eq. (2)) for Palm, assuming that the seedling density of Palm is similar to that of Early—decreasing with time since disturbance—but with different starting seedling level (n_0) and decaying factor (α). We tested 36 combinations of n_0 varying from 0 to 0.05 individuals m^{-2} yr^{-1} with interval 0.01 individuals m^{-2} yr^{-1} and α varying from 0 to 0.05 yr^{-1} with interval 0.01 yr^{-1}. We found that five of them lead to a smaller *MSE* (Eq. (3)) than the GLUE optimal simulation (0.1678, 0.1662, 0.1642, 0.1646, and 0.1691 for the five experiments and 0.1803 for the GLUE optimal), and the five combinations have the same starting seedling density (n_0=0.02 individuals m^{-2} yr^{-1}) but different values of the decaying factor (α=0.01, 0.02, 0.03, 0.04, and 0.05 yr^{-1}, respectively) (Figure S7). To choose from the five decaying values, we compared the recovery density schemes with the observed recruitment of Palms. There were 37, 64, 50, 34, and 32 palms recruited in the 85 plots (78.5 m^2 each plot) in 1994, 1999, 2004, 2009, and 2014 censuses, respectively, which corresponds to 0.0011, 0.0019, 0.0015, 0.0010, and 0.0010 individuals m^{-2} yr^{-1} after 5, 10, 15, 20, and 25 years of the Hugo disturbance. In other words, the recruitment decreases to half of the starting level in 20–25 years, or a decaying factor $\alpha \approx 0.03$ yr^{-1}. We assume that the seedling density has the same decaying rate as the recruitment density and thus we select the seedling density scheme n_0=0.02 individuals m^{-2} yr^{-1} and α=0.03 yr^{-1} as the seedling recovery scheme for Palm.

After changing the aging mortality of Palm to zero and the seedling density to a lower and slowly decreasing value, we did not repeat the GLUE. This is because Palm has constrained DBH size (between 10 and 25 cm) and decreasing the aging mortality increases its density while decreasing seedling reproduction decreases its density, which maintains the overall density of Palm, without affecting other variables of Palm nor variables of other PFTs (Figure S7). Therefore, we use the parameter set found from the GLUE (Table 1) but with 0-aging mortality and a lower seedling density recovery (n_0=0.02 individuals m^{-2} yr^{-1} and α=0.03 yr^{-1}) for simulations in the following studies.

https://doi.org/10.5194/gmd-2021-410
Preprint. Discussion started: 14 January 2022

Geoscientific Model Development Discussions

2.4 Parameter Sensitivity Analyses and Variance Decomposition

Using a similar approach to PEcAn (LeBauer et al. 2013), we analyze the sensitivity of model simulations to the parameters and the contribution of the parameters to the variances. Specifically, we set up nine experiments for each of the 41 parameters, corresponding to the nine quantiles (10^{th}, 20^{th}, …, 90^{th}) of the posterior distribution of each parameter, while all other parameters remain constant at their optimal. For the total 369 sensitivity experiments, we initialize the model with the pre-Hugo observation and run each experiment for 25 years (1989–2014).

To study the stability of the optimal parameter set, we calculate the *MSE* of each experiment and compare it with the *MSE* of the optimal. To quantitively study the sensitivity of output variables to the parameters, we calculate the standardized cubic regression coefficient (β),

$$\beta = \frac{\partial \tilde{x}(p_o)}{\partial p_o} \Big/ \frac{x_o}{p_o}, \tag{7}$$

where p and x are a specific parameter and the corresponding output variable. $\tilde{x}$ is the cubic regression function of x on p: $\tilde{x} = ap^3 + bp^2 + cp + d$, estimated from the pairs of parameter p and variable x along the nine quantiles of the posterior distribution of parameter p. $\frac{\partial \tilde{x}(p_o)}{\partial p_o}$ is the partial derivative of $\tilde{x}$ on p at p_o, where p_o and x_o are the optimal value of the parameter and the corresponding output variable. Only when the R^2 metrics of the regression function is significant at 99% confidence level via student-t test is β calculated. We calculate β for 20 variables [stem density, BA, AGB, and leaf area index (LAI) of each PFT and of all PFTs] and for the 41 parameters. The β for the variables at the first and the 25^{th} simulation years are selected to represent the short-term and long-term response of modeled variables to the parameters, respectively.

To quantitatively study the uncertainty of the simulated variables (stem density, AGB, BA, LAI, etc.) from the uncertainties of the parameters, we calculate the coefficient of variation (θ) for each variable resulting from experiments with different parameters:

$$\theta = \frac{\sigma}{\mu}, \tag{8}$$

where σ and μ are the standard deviation and the mean value of the variable from the nine experiments of the parameter. To study the contribution of each parameter to the uncertainties of the simulated variables, we calculate the total variance from all the sensitivity experiments (Var_T) and the variance from experiments of each parameter (Var_p), and decompose the total variance as follows,

$$Var_T = \sum_{p=1}^{Np} Var_p + \omega\,, \tag{9}$$

where Var_p is the variance of the model outputs from experiments with different values of parameter p, and Np is the total number of parameters (Np=41), ω represents the variance from the interaction among parameters.

2.5 Experiments with Different Initial Conditions

To study the impact the initial condition of the forest on the recovery, we set up two experiments with different initial forest states (pre-Hugo state and pre-Maria state) with a hurricane disturbance in the first simulation year (experiment IhugoH1 and experiment ImariaH1, hereafter), and one control experiment with pre-Hugo state and no hurricane

https://doi.org/10.5194/gmd-2021-410
Preprint. Discussion started: 14 January 2022


Geoscientific Model Development Discussions

disturbance in all simulation years (experiment IhugoHn, hereafter). The three experiments run for 112 simulation years (corresponding to years 1989–2100). The meteorological drivers between 1989 and 2017 are observations from meteorological towers at BEW, and the meteorological drivers between 2018 to 2100 are randomly sampled from the observations between 1989 and 2017. Hurricane disturbance is turned off in all simulation years for experiment IhugoHn and in all but the first simulation year for experiments IhugoH1 and ImariaH1. Thus, experiment IhugoHn represents the succession of the forest without hurricane disturbances for more than a century. Experiments IhugoH1 and ImariaH1 represent the recovery of the forest from a hurricane disturbance given different initial conditions of the forest.

3 Results

3.1 Model Assessment

3.1.1 Optimal Simulation and Optimal Parameter Set

Figure 3 shows the optimal model simulation along with census observations for years 1989–2018. The simulated stem density of Early increased from 0.0027 individuals m^{-2} in 1990 to 0.0324 in 1994 (1100% increase) and to 0.0748 in 1999 (131% increase) and decreased steadily thereafter, consistent with observations (0.0030 individuals m^{-2} in post-Hugo 1989, 1673% increase in 1994 and 84% increase in 1999). The simulated stem density of Mid is overall underestimated by 47% compared to the mean from the 85 plots of observations, but is within one standard deviation of the observations. The simulated stem density of Late and Palm are also consistent with observations with 25% underestimation and 38% overestimation, respectively. The optimal simulation overestimates the growth rate of the Early PFT by 133% for years between 2000 and 2014, but it generally captures the decrease of growth rate with time since the hurricane disturbance for all PFTs. Furthermore, the optimal simulation agrees well with the observations for the overall stem density (-21% relative bias), basal area (-12% relative bias), and aboveground biomass (-15% relative bias), and captures well the PFT composition (+1%, -8%, -2%, and +9% differences in the percentages of Early, Mid, Late, and Palm PFTs, respectively) and size structure (+0.8% differences in the percentage of large stems) (Figure 4).

https://doi.org/10.5194/gmd-2021-410
Preprint. Discussion started: 14 January 2022

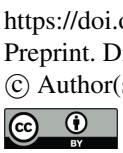

Geoscientific Model Development Discussions
Open Access
EGU

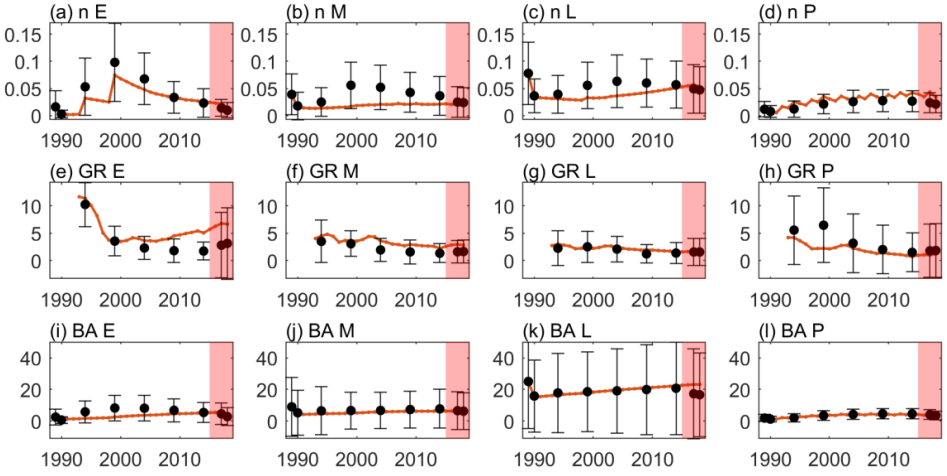

Figure 3. Time series of variables from observation and the optimal simulation. (a)-(d) stem density of all trees (n; DBH ≥ 2.5 cm) (individuals m^{-2}) for Early, Mid, Late, and Palm PFTs, respectively. (e)-(h) diameter growth rate (GR; cm $(5yrs)^{-1}$) for the four PFTs; (i-l) basal area (BA; cm^2 m^{-2}) for the four PFTs. The dots and the error bars represent the means and the one standard deviations from the means. Period between 1989–2014 is for model calibration and period between 2015–2018 is for model validation (shaded).

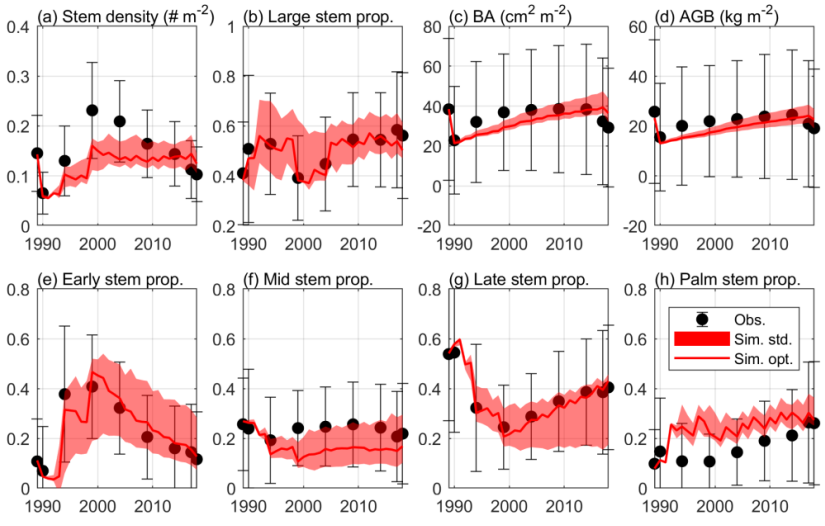

Figure 4. The standard deviation of the estimated variables with K=8 in equation (4), along with the optimal simulation and observation. The figure shows (a) stem density of all stems with DBH ≥ 2.5 cm (individuals m^{-2}), (b) stem density proportion of large stems with DBH ≥ 10 cm, (c) basal area (BA; cm^2 m^{-2}), (d) aboveground biomass (AGB; kgC m^{-2}), and stem density proportion of (e) Early, (f) Mid, (g) Late, and (h) Palm PFTs.

In the verification period between 2015–2018, the simulated overall stem density, basal area, and aboveground biomass have a relative bias of +24%, +23%, and +17%, respectively, compated to the mean of the observations. The simulated percentages of the four PFTs have a difference of +3%, -7%, -4%, and 8%, respectively;

https://doi.org/10.5194/gmd-2021-410
Preprint. Discussion started: 14 January 2022

Geoscientific Model Development Discussions

and the simulated large stem percentage has a difference of +0.3% compared to the mean of the observations. Overall, the simulated variables between 2015–2018 are within the standard deviations of the observations (Figure 3 and Figure 4), suggesting that the parameters found using the data between 1989–2014 are valid for the 2015–2018.

Table 1 shows the optimal set of the parameter values. The clumping factor (0.34) is lower than that from other studies in different locations (~0.7; He et al. 2012). Other parameters are reasonable and are consistent with reported values. For example, the leaf turnover rate of Late (0.16 $year^{-1}$) is consistent with a previous study (~0.1; Gill and Jackson 2000). The leaf turnover rate of Palm (0.42 $year^{-1}$) is consistent with previous observations of 0.36 $year^{-1}$ at BEW (Lugo et al. 1998). The woody tissue density of Palm (0.24 g cm^{-3}) is consistent with previous observations of 0.25 g cm^{-3} for the palm species *Prestoea decurrens* (Zanne et al. 2009; Chave et al. 2009) that is the same genus as the palm species at our study site.

Table 1. The optimal parameter set obtained from the GLUE method.

Parameter Name	Units	Early	Mid	Late	Palm
clumping factor (Clf)	proportion	0.34			
fine root allocation (FRA)	ratio	0.64	1.2	0.95	1.85
leaf turnover rate (LTR)	$year^{-1}$	1	0.83	0.16	0.42
leaf width (LWd)	m	0.1	0.07	0.16	0.13
quantum efficiency (Qef)	$mol_{CO2}\ mol^{-1}_{photon}$	0.055	0.069	0.038	0.05
dark respiration rate (Rdf)	proportion	0.0071	0.0144	0.0143	0.0088
growth respiration rate (Rgf)	ratio	0.44	0.595	0.421	0.401
specific leaf area (SLA)	m^2kg^{-1}	23.26	22.28	13.19	14.15
stomatal slope (SSp)	ratio	6.17	8.02	5.35	5.07
carboxylation rate (Vm0)	$\mu mol_{CO2}\ m^{-2}s^{-1}$	23.32	21.73	9.29	12.24
wood density (WDe)	$10^3\ kgm^{-3}$	0.32	0.6	0.77	0.24

3.1.2 Posterior Distribution of Parameters

Figure 5 shows the posterior and prior probability distribution functions (PDFs) of the parameters. The most significant differences between the posterior and the prior distributions are for the parameters of clumping factor (Clf) and dark respiration rate (Rdf). The posterior PDFs of some parameters (i.e., carboxylation rate, specific leaf area, leaf width, stomatal slope, and wood density) do not change much from the priors (the maximum difference between the prior and posterior CDFs is generally less than 0.1) because the prior distributions of those parameters are well constrained by observational trait data (Feng et al. 2018). The posterior PDFs of other parameters (e.g., leaf turnover rate, quantum efficiency, and fine root allocation), especially for the Early and Mid PFTs, with few observational trait data (Feng et al. 2018), changed greatly from the prior distributions (the maximum difference between the distributions is around 0.3).

https://doi.org/10.5194/gmd-2021-410
Preprint. Discussion started: 14 January 2022

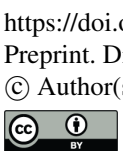

Geoscientific Model Development Discussions

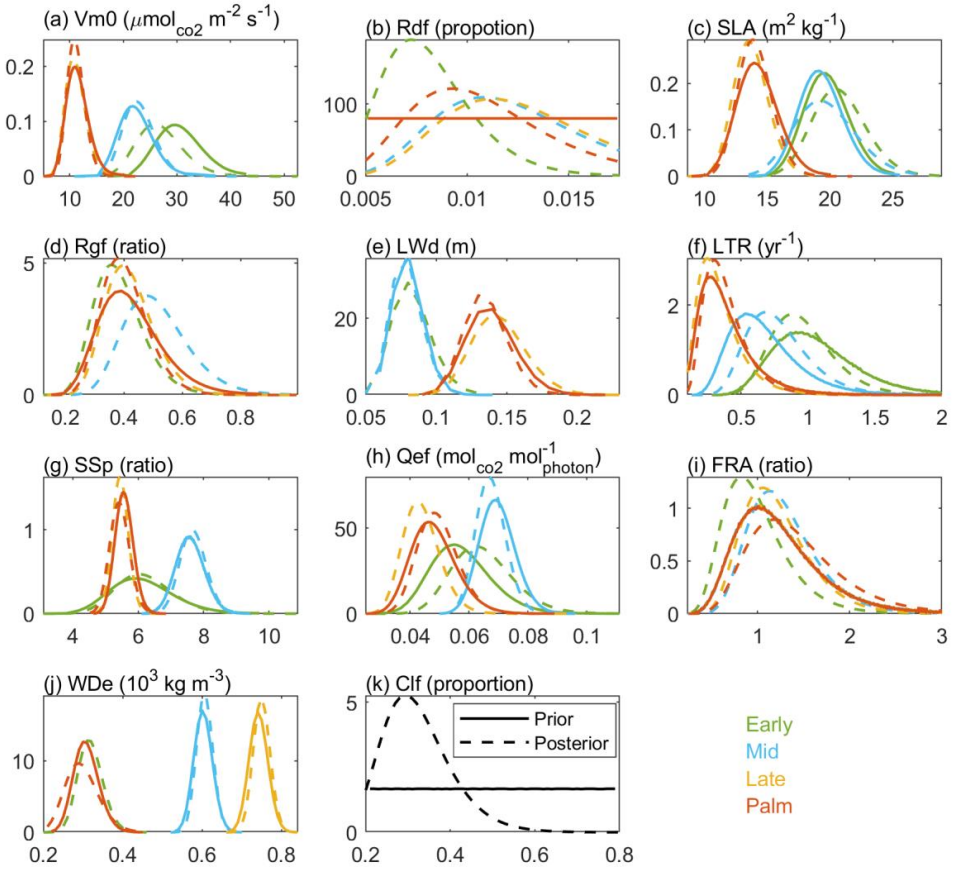

366

367 **Figure 5.** The prior (solid line) and posterior (dashed line) probability density functions for the four PFTs (colors) of the 11
368 parameters. The first ten parameters are PFT-dependent, and the last one leaf clumping factor (Clf) is PFT-independent. Palm has
369 the same prior distribution as Late for all parameters except that the wood density (WDe) of Palm has the same prior distribution
370 as that of Early. The long name of each parameter is shown in Table 1.

371

372 ### 3.1.3 Parameter Sensitivity and Uncertainty

373 Among the 369 sensitivity experiments with different parameter values, 57 of them have slightly smaller *MSE*s than
374 the optimal, but the simulated variables (stem density, AGB, PFT composition, and size structure) from those
375 experiments are very close to those from the optimal (Figure S8), indicating that the optimal simulation we found
376 from GLUE is stable given the uncertainties of the parameters.

377 In terms of the sensivitiy of simulated variables on the parameters, the magnitude of standardized cubic
378 regression coefficients (β) are generally low (~0.2) in the first simulation year (Figure 6 a), indicating that the
379 parameters do not have strong effect on the variables. LAI is the most sensitive variable in the short term, and it is
380 sensitive to both the specific leaf area (SLA) of its own PFT and the clumping factor (Clf). Furthermore, each PFT is

https://doi.org/10.5194/gmd-2021-410
Preprint. Discussion started: 14 January 2022

Geoscientific Model Development Discussions

mainly sensitive to the parameters of its own PFT, and vice versa (Figure 6 a). After 25 years of simulation, the sensitivity of the variables on the parameters becomes more complex (Figure 6 b). First, the magnitude of β increases significantly, indicating that the parameters show stronger impacts on the variables in the long term. Second, the variables are sensitive to different parameters in the short term and in the long term. For example, SLA and clumping factor are the most important parameters to LAI in the first simulation year, but not after 25 years of simulation. Instead, quantum efficiency (Qef) and dark respiration (Rdf) are the most important parameters to LAI after 25 years of simulation. Third, besides the sensitivity of variables to the parameters of their own PFT, variables of a specific PFT also show sensitivity to the parameters of other PFTs. For example, the variables of Early and Mid PFTs are not only sensitive to Early and Mid PFTs parameters, but also sensitive to Late PFT parameters. Specifically, the quantum efficiency, wood density, and specific leaf area have significant positive effects on the variables of its own PFT, but significant negative effects on other PFTs. The Palm PFT is sensitive to its own parameters, but also to the specific leaf area of the Early PFT (Figure 6 b).

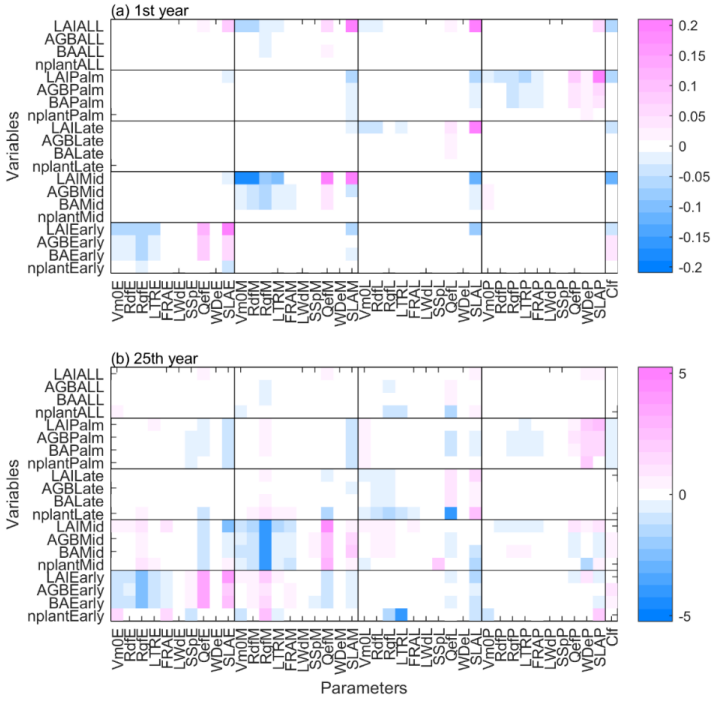

Figure 6. The standardized cubic regression coefficient (β) of variables at (a) first and (b) 25th year of the simulations regarding to the parameters. The variables include stem density (nplant), basal area (BA), aboveground biomass (AGB), and leaf area index (LAI) for each PFT. The parameters include 10 PFT-dependent parameters and one PFT-indipendent parameter listed in Table 1.

The stem density has a larger variation than LAI, BA and AGB after 25 years of simulation (Figure 7). Given that large stems contribute more to LAI, BA, and AGB, larger variation of stem density than LAI, BA, and AGB indicates that small stems are more variable than large stems. The variation of those variable also varies with PFTs.

https://doi.org/10.5194/gmd-2021-410
Preprint. Discussion started: 14 January 2022

Geoscientific Model Development Discussions

For the stem density, Late PFT has the largest variation, followed by Early, then Mid, and Palm has the smallest variation, indicating that stem density of small Late is the most sensitive to the uncertainty of the parameters. For BA, AGB, and LAI, Early and Mid PFTs show the highest variability, followed by the Palm PFT, and the Late PFT has the lowest variation, indicating that large stems of Early and Mid PFTs are more sensitive to the uncertainty of the parameters than large stems of Late and Palm PFTs.

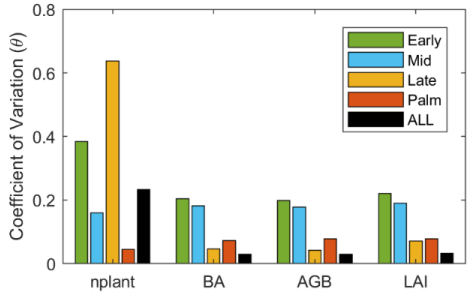

Figure 7. The coefficient of variation (θ) for the variables of each PFT at the 25th simulation year.

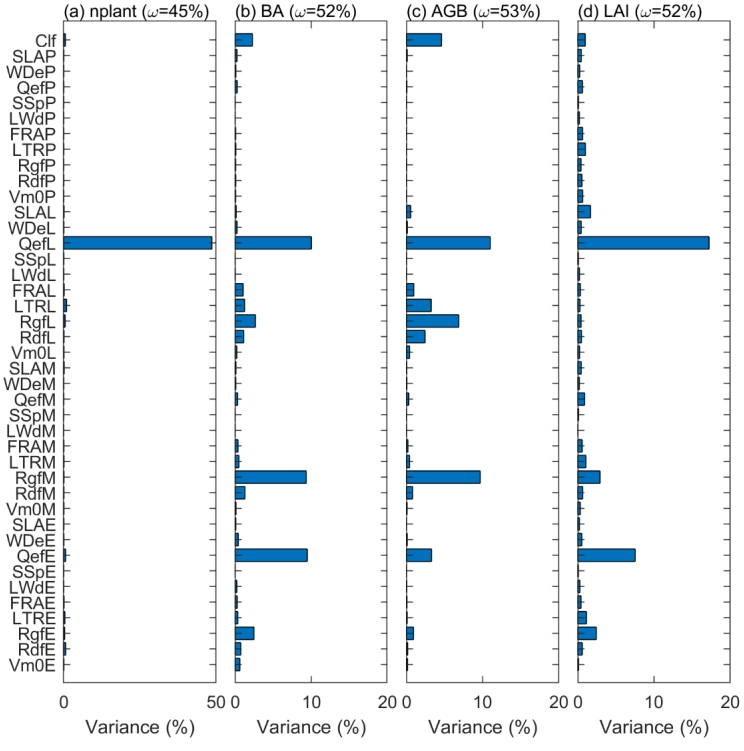

Figure 8. The variance explained by each parameter for variables (a) stem density, (b) basal area, (c) aboveground biomass, and (d) leaf area index. The variance explained by the interaction among parameters are given in the parenthesis.

https://doi.org/10.5194/gmd-2021-410
Preprint. Discussion started: 14 January 2022

Geoscientific Model Development Discussions

413 The variance decomposition analyses reveal that 50% of the uncertainty of the stem density comes from the
414 quantum efficiency of Late (QefL) (Figure 8). However, QefL explains less than 10% of the uncertainty in BA, AGB,
415 and LAI, indicating that QefL has significant effects on the density of small stems, but less effects on the density of
416 large stems. In other words, QefL impacts the recruitment and establishment of stems more than the growth of stems.
417 The uncertainty of the growth of stems come from the growth respiration factor (Rgf), which explains about 10% of
418 the uncertainty. The interaction among parameters accounts for 21% of the uncertainty of the stem density, and more
419 than 50% of the uncertainty of the BA, AGB, and LAI.

420 **3.2 Impact of Initial Condition on Forest Recovery**

421 Figure 9 shows the 112-year simulations of the forest initialized with different forest states (pre-Maria state and pre-
422 Hugo state) with or without hurricane disturbance at the first simulation year. Without hurricane disturbance
423 (IhugoHn), the forest experiences a decrease (-17%) in stem density in the first 10 years due to the self-thinning
424 process of the forest (Figure 9 a). The decrease is mainly attributed to mortality of small stems of Mid and Late PFTs
425 (Figure S9 b and c), which leads to an increase (5%) in the proportion of large stems (DBH ≥ 10 cm) (Figure 9 b) but
426 BA and AGB remain steady (Figure 9 c and d). After 10 years, a large number of Early PFT stems recruit with DBH
427 less than 10 cm (Figure S9 a), decreasing the overall large stem proportion. After 30 years, Mid trees recruit and grow
428 (Figure S9 b and Figure S10 b), increasing the total BA and AGB (Figure 9 c and d). As small Late trees recruit
429 frequently after 20 years (Figure S9 c), the stem density increases steadily, and the proportion of large stems decreases
430 steadily. Because small stems contribute little to BA and AGB, BA and AGB have a slower increase with time (Figure
431 9 c and d) than stem density (Figure 9 a).

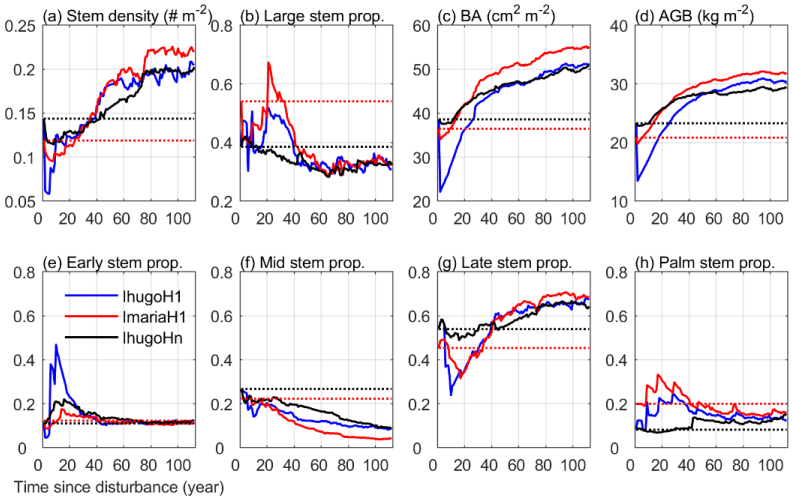

432

433 **Figure 9.** Time series of eight variables from the simulation of the three experiments: IhugoHn, IhugoH1, ImariaH1. The dotted
434 lines are the initial state of the variables for each experiment (IhugoHn and IhugoH1 have the same initial state). The variables in
435 (a) stem density, (c) basal area, and (d) aboveground biomass are for stems with DBH ≥ 2.5 cm. The stem proportion in (b) is the
436 propotion of the stem denisty with DBH ≥ 10 cm to the stem denisty with DBH ≥ 2.5 cm. The variables in (e)-(h) are the proportion
437 of the stem density of each PFT with DBH ≥ 2.5 cm to the total stem density of all PFTs with DBH ≥ 2.5 cm.

438

https://doi.org/10.5194/gmd-2021-410
Preprint. Discussion started: 14 January 2022

Geoscientific Model Development Discussions

After 80 years, the PFT composition reaches a steady state, where the Early, Mid, Late, and Palm PFTs account for 11.8%, 10.6%, 65.3%, and 12.3% of the total stem density, respectively (Figure 9 e, f, g, h). This state is significantly different from the initial state and exhibits a 16% reduction on the proportion of the Mid PFT. It exhibits increases on all other PFTs proportions (+0.7%, +11.4%, and +4.1% for Early, Late, and Palm, respectively). The Early PFT has stems of all DBH classes (Figure S9 a); while Mid PFT has mostly small stems with DBH less than 5 cm and a small cohort (2 individuals ha^{-1}) of large stems with DBH around 200 cm (Figure S11 b and f), which contributes a significant portion to the total AGB (Figure S10 b). The Late PFT is the most abundant PFT (Figure S9 c) and contributes the most to the total AGB in the forest (Figure S10 c). The stem density of Late decreases with DBH (Figure S9 c), and the largest-DBH cohort reaches 180 cm (Figure S11 c), which is smaller than that of Mid but has a higher density (7 individuals ha^{-1}) (Figure S11 g). The maximum DBH is far larger than that we observed (89 cm in 2017) but is possible given 100 years of growth with a 2 cm yr^{-1} increment in DBH (Brandeis 2009). Palm recruits with DBH between 10 and 15 cm, the DBH grows slowly after recruitment, and DBH growth stops after they reach the reproduction height (18 m, and 25 cm in DBH correspondingly) and allocate all carbon to reproduction (Sect. 2.1.2), hence palms do not exceed 25 cm DBH (Figure S11 d) and most of them are between 10 and 20 cm (Figure S9 d and Figure S10 d). This is in agreement with the maximum reported values of DBH (Lugo and Rivera Batlle 1987).

Compared with the experiment without hurricane disturbance in the first simulation year (IhugoHn), the ones with hurricane disturbance in the first simulation year (IhugoH1 and ImariaH1) reach higher BA and AGB levels after 60 years of succession from the hurricane disturbance (Figure 9 c and d). This is due to the carbon accumulation of large Late PFT in disturbed forests (Figure S10 g and k). Large Late trees in disturbed forest (IhugoH1 and ImariaH1) have higher growth rate and lower background mortality rate compared to those in the undisturbed forest (IhugoHn) (Figure 10) because of the decreased competition to reach the open canopy. As the disturbed forest recovers, the BA and AGB increase to the level of the undisturbed forest (Figure 9 c and d), the growth rate decreases (Figure 10 a) and the mortality rate increases to the levels of those in the undisturbed forest, especially for severely disturbed forest (IhugoH1) (Figure 10). With lower mortality and higher growth rate in the first 60 years, there will be more large Late trees in the canopy at the end of the simulation (12 individuals ha^{-1} vs 8 individuals ha^{-1}) (Figure S11 g) even though the maximum DBH will be smaller (Figure S11 c).

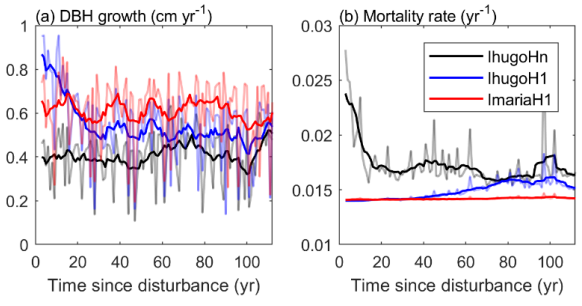

Figure 10. Times series of (a) growth rate and (b) mortality rate of Late trees with DBH ≥ 20 cm. The light-colored lines represent the yearly values, and the solid lines are ten-year moving averages.

https://doi.org/10.5194/gmd-2021-410
Preprint. Discussion started: 14 January 2022


Geoscientific Model Development Discussions

The recovery is different with different initial states. With pre-Hugo state (IhugoH1), the forest takes 25 years to recover to the pre-disturbance BA and AGB levels (Figure 9 c and d), but with pre-Maria state (ImariaH1), it takes only 10 years to recover to the pre-disturbance BA level (Figure 9 c) and 5 years to the pre-disturbance AGB level (Figure 9 d). The succession dynamics are different, too. With pre-Hugo state, the hurricane-induced mortality is very high, and thus the canopy opens, and Early and Palm PFTs recruit greatly in the first 20 years (Figure S9 e and h), and then it is taken over by the Late PFT (Figure S9 g). With pre-Maria initial state, the hurricane-induced mortality is low, and the canopy is not significantly changed after the hurricane, and Early PFT does not recruit as much as it does in the pre-Hugo state initialized simulation (Figure S9 i and e). The PFT composition after 100 years is similar for the two simulations, but the BA and AGB is not (Figure 9). The BA and AGB with the pre-Maria initialization are higher than those with the pre-Hugo initialization throughout the 110 years of simulations, even though the initial AB and AGB levels in the pre-Maria state are lower than those in the pre-Hugo state (Figure 9 c and d). This is because of the higher mortality at the first year with pre-Hugo state, leading to a larger reduction in the density of large stems. With the succession following the disturbance, there are more large stems, especially Late and Palm, in the pre-Maria simulation than in the pre-Hugo simulation (Figure S11), contributing to the higher AGB and BA in the pre-Maria simulation (Figure S10 g, h, k, and l).

4 Discussion

4.1 Limitations and Advantages of GLUE

GLUE samples from continuous distributions, but the sampled parameter sets are in a discrete space, therefore, the GLUE approach may not lead to the true optimum due to the finite number of samples. To justify the sample size of 10,000 for 41 parameters in this study, we repeated GLUE for a larger sample size (20,000). The optimal simulation from 20,000-sample GLUE (Figure S12) is very similar to that from the 10,000-sample GLUE (Figure 3) and the optimal parameter sets from the two GLUEs are similar, suggesting that the two GLUEs found an optimum around the same local optimum and 10,000 samples are sufficient for the 41 parameters. However, given the nature of equifinality, there may be multiple parameter sets that can lead to the same observed state (Beven and Freer 2001), and thus the optimal parameter set we found from GLUE may be one of many possible solutions.

Although GLUE may not guarantee the global optimum, it implicitely handles any effects of model nonlinearity, model structure errors, input data errors, and parameters covariation (Beven and Freer 2001). Moreover, GLUE allows us to optimize parameters using any variables of interests in the cost function. For example, in our study, we want to make sure the model captures the size structure and PFT composition of the forest community, and thus we utlized forest stand variables including stem density, growth rate, and BA of each PFT in the cost function. Compared to other optimizers (such as PEcAn) that calibrates parameters using plant traits observations (e.g., wood density, leaf turnover rate), GLUE's ability of utlizing observations of forest stand variables (BA, AGB, etc.) could further reduce the uncertainty of parameters (Wang et al. 2013). Note that we did not calibrate the parameters using plant traits observations in this study, because the parameters we use are already calibrated with plant traits observations in Feng et al. (2018) and we adpoted their calibrated parameters in our study (see Sect. 2.3.1).

https://doi.org/10.5194/gmd-2021-410
Preprint. Discussion started: 14 January 2022


Geoscientific Model Development Discussions

4.2 Uncertainty of Model Outputs from Parameters

To be consistent with census observations, we included stems with DBH ≥ 2.5 cm in the analyses. The large variation of simulated stem density (Figure 7) could be due to the timing of cohorts exceeding the 2.5 cm threshold, and thus can be minimized by averaging stem density over several years (Massoud et al. 2019). LAI is generally underestimated in the vegetation dynamic models (e.g., Xu et al. 2016). As shown in Figure 6, the clumping factor is one of the most important parameters controlling LAI. However, both LAI and the clumping factor are rarely measured and LAI estimated from satellite remote sensing data often have variable quality, especially in tropical forests (Xiao et al. 2016, 2017). Future census practices should include LAI and clumping factor. Even though the LAI measured from the ground may be different from the LAI measured from above the canopy (airborne lidar or satellites), ground measurements could provide useful information for both the vertical structure of the forest and the quality of satellite remote sensing and airborne lidar data. The clumping factor we calibrated for our study site is lower than that from other locations (He et al. 2012). Observations of clumping factor in our study site are needed to verify the parameter from our model calibration and improve model estimates of LAI.

Out results agree with a previous study that modeled variables have different response to parameters in the short term (e.g., first simulation year) and in the long term (e.g., 25th simulation year) (Massoud et al. 2019). Furthermore, we showed that variables of a specific PFT are most sensitive to the parameters of the same PFT, but also sensitive to parameters of other PFTs. Those interactions between variables and parameters indicates the competition among PFTs. For example, Palm is sensitive to its own parameters, but also to Early SLA. This can be explained by the competition for light between Early and Palm, where a higher SLA of Early PFT leads to a higher LAI of Early allowing Early to photosynthesize more efficiently and thus be more competitive in the community. Those competitions are important for the co-existence of PFTs in model simulations and critical to the PFT composition and succession.

5 Conclusion

Hurricanes are a major disturbance to tropical forests, but hurricane disturbance has not been implemented in any model of vegetation dynamic. In this study, we implemented hurricane disturbance in the Ecosystem Demography model (ED2) and calibrated the model with forest stand observations of a tropical forest in Puerto Rico. The calibrated model has good representation on the recovery trajectory of PFT composition, size structure, stem density, basal area, and aboveground biomass of the forest. We used the calibrated model to study the recovery of the forest from a hurricane disturbance with different initial forest states, and found that a single hurricane disturbance changes forest structure and composition in the short term and enhances AGB and BA in the long term compared with a no-hurricane situation. Forests with wind-resistant initial state will have lower mortality, recover faster, and reach a higher BA and AGB level than forests with a less wind-resistant initial state.

The model developed and results presented in this study can be utilized to understand the fate of tropical forests under a changing climate. Hurricanes are likely to become more frequent and severe in the future with global warming (IPCC 2021). With frequent hurricane disturbances in the future, forests will not have enough time to reach

https://doi.org/10.5194/gmd-2021-410
Preprint. Discussion started: 14 January 2022

a steady state, and the structure and composition will be constantly changing, which provides different initial states for future hurricane disturbances and thus different recovery trajectories. Climate change with changing temperature, precipitation, and CO_2 concentration, etc. will also have an impact on the growth of individual trees and thus the structure and composition of forests (e.g., Feng et al. 2018). The ED2-HuDi model developed in this study will be a beneficial tool to understand the impact of frequent hurricane disturbances on forest recovery in the future under the changing climate.

Code and data availability. The ED2-HuDi software are publicly available. The most up-to-date source code is available at https://github.com/zhjiay5/ED2. The exact version used in this paper is archived on Zenodo (https://dx.doi.org/10.5281/zenodo.5565063). Input data and scripts to run the model and produce the plots for all the simulations presented in this paper are also publicly available at http://www.hydrology.gatech.edu/.

Author contributions. R.L.B. conceptualized the work, T.H.S provided field data and contributed ecological perspectives, R.L.B. and J.Z. developed the methodology and performed the analyses, J.Z. and M.L. interpreted results, J.Z. wrote the first draft of the manuscript. All authors discussed results, and critically revised and edited the manuscript.

Competing interests. Authors declare no competing interests.

Acknowledgements. We thank Paul Moorcroft, Xiangtao Xu, Elsa Ordway, Félicien Meunier and Erik Larson for discussions on the model implementation and parameter sensitivity analyses. We acknowledge high-performance computing support from Cheyenne (doi:10.5065/D6RX99HX) provided by NCAR's Computational and Information Systems Laboratory, sponsored by the National Science Foundation. This work was supported by National Science Foundation (project EAR1331841) and K. Harrison Brown Family Chair. The USDA Forest Service International Institute of Tropical Forestry works in collaboration with the University of Puerto Rico. The research was carried out at the Jet Propulsion Laboratory, California Institute of Technology, under a contract with the National Aeronautics and Space Administration. M.L. was supported by the NASA Postdoctoral Program, administered by Universities Space Research Association under contract with NASA, and by the Next Generation Ecosystem Experiments-Tropics, funded by the U.S. Department of Energy, Office of Science, Office of Biological and Environmental Research.

References

Albani, M, Medvigy, D., Hurtt, G. C., and Moorcroft, P. R.: The controbutions of land-use change, CO_2 fertilization, and climate variability to the Eastern US carbon sink, Global Change Biology, 12, 2370–2390, 2006.

Baraloto, C. et al.: Decoupled lead and stem economics in rain forest trees, Ecology Letters, 13, 1338–1347, 2010.

Beven, K. and Binley, A.: The future of distribution models: Model calibration and uncertainty prediction, Hydrological Processes, 6, 279–298, 1992.

https://doi.org/10.5194/gmd-2021-410
Preprint. Discussion started: 14 January 2022

576 Beven, K. and Freer, J.: Equifinality, data assimilation, and uncertainty estimation in mechanistic modelling of
577 complex environmental systems using the GLUE methodology, Journal of Hydrology, 249, 11–29, 2001.
578 Binley, A. M. and Beven, K. J.: "Physically-based modelling of catchment hydrology: a likelihood approach to
579 reducing predictive uncertainty", in: Computer Modelling in the Environmental Sciences, edited by: Farmer,
580 D. G. and Rycroft, M. J., Clarendon Press, Oxford, 75–88, 1991.
581 Brandeis, T. J.: Diameter growth of subtropical trees in Puerto Rico, Res. Pap. SRS–47. Asheville, NC: U.S.
582 Department of Agriculture Forest Service, Southern Research Station. 39 pp., 2009.
583 Brokaw, N. V. L.: *Cecsropia schreberiana* in the Luquillo Mountains of Puerto Rico, Botanical Review, 64, 91–120,
584 https://www.jstor.org/stable/4354318, 1998.
585 Chambers, J. Q., Fisher, J. I., Zeng, H., Chapman, E. L., Baker, D. B., and Hurtt, G. C.: Hurricane Katrina's carbon
586 footprint on U.S. Gulf Coast Forests, Science, 318, 1107, 2007.
587 Chave, J., Coomes, D. A., Jansen, S., Lewis, S. L., Swenson, N. G., and Zanne, A. E.: Towards a worldwide wood
588 economics spectrum, Ecology Letters, 12, 351–366, 2009.
589 Chen, J. and Black, T.: Foliage area and architecture of plant canopies from sunfleck size distributions, Agricultural
590 and Forestry Meteorology, 60, 249–266, 1992.
591 Cole, L. E. S., Bhagwat, S. A., and Willis, K. J.: Recovery and resilience of tropical forests after disturbance, Nature
592 communications, 5, 3906, 2014.
593 Curran, T. J., Gersbach, L. N., Edwards, W., and Krockenberger, A. K.: Wood density predicts plant damage and
594 vegetative recovery rates caused by cyclone disturbance in tropical rainforest tree species of North
595 Queensland, Australia, Austral Ecology, 33, 442–450, 2008.
596 di Porcia e Brugnera, M. et al.: Modeling the impact of liana infestation on the demography and carbon cycle of
597 tropical forests, Global Change Biology, 25, 3767–3780, 2019.
598 Everham, M. E. III and Brokaw, N. V. L.: Forest damage and recovery from catastrophic wind, The Botanical Review,
599 62, 2, 113–185, 1996.
600 Feng, X. et al.: Improving predictions of tropical forest response to climate change through integration of field studies
601 and ecosystem modeling, Global Change Biology, 24, e213–e232, 2018.
602 Fisher, R. A. and Koven, C. D.: Perspectives on the future of Land Surface Models and the challenges of representing
603 complex terrestrial systems, Journal of Advances in Modeling Earth Systems, 12, e2018MS001453, 2020.
604 Fisher, R. A. et al.: Vegetation demographics in Earth System Models: A review of progress and priorities, Global
605 Change Biology, 24, 35–54, 2018.
606 Francis, J. K. and Gillespie, A. J. R.: Relating gust speed to tree damage in hurricane Hugo, 1989, Journal of
607 Arboriculture, 19, 368–373, 1993.
608 Freer, J., Beven, K., and Ambriose, B.: Bayesian estimation of uncertainty in runoff prediction and the value of data:
609 An application of the GLUE approach, Water Resources Research, 32, 2161–2173, 1996.
610 Gill, R. A. and Jackson, R. B.: Global patterns of root turnover for terrestrial ecosystems, New Phytologist, 147, 13–
611 31, 2000.

https://doi.org/10.5194/gmd-2021-410
Preprint. Discussion started: 14 January 2022

612 Gregory, A. A and Sabat, A. M.: The effect of hurricane disturbance on the fecundity of sierra palms (Prestoea
613 montana), Bios, 67, 135–139, 1996.
614 Hall, J., Muscarella, R., Quebbeman, A., Arellano, G., Thompson, J., Zimmerman, J. K., and Uriarte, M.: Hurricane-
615 induced rainfall is a stronger predictor of tropical forest damage in Puerto Rico than maximum wind speeds,
616 Scientific Reports, 10, 4318, 2020.
617 He, L., Chen, J. M., Pisek, J., Schaaf, C. B., and Strahler, A. H.: Global clumping index map derived from the MODIS
618 BRDF product, Remote Sensing of Environment, 119, 118–130, 2012.
619 Heartsill Scalley, T.: Insights on forest structure and composition from long-term research in the Luquillo mountains,
620 Forests, 8, 204, 2017.
621 IPCC: Climate Change 2021: The physical science basis. Contribution of Working Group I to the Sixth Asscessment
622 Report of the Intergovernmental Panel on Climate Change [Masson-Delmotte, V. et al. (eds.)]. Cambridge
623 Unveristy Press, 2021, In Press.
624 LeBauer, D. S., Wang, D., Richter, K. T., Davidson, C. C., and Dietze, M. C.: Facilitating feedbacks between field
625 measurements and ecosystem models, Ecological Monographs, 83, 133–154, 2013.
626 Leitold, V. et al.: Tracking the rates and mechanisms of canopy damage and recovery following hurricane Maria using
627 multitemporal Lidar data, Ecosystems, https://doi.org/10.1007/s10021-021-00688-8, 2021.
628 Lewis, R. J. and Bannar-Martin, K. H.: The impact of cyclone Fanele on a tropical dry forest in Madagascar,
629 Biotropica, 44, 135–140, 2011.
630 Longo, M. et al.: The biophysics, ecology, and biogeochemistry of functionally diverse, vertically and horizontally
631 heterogeneous ecosystems: the Ecosystem Demography model, version 2.2 – part 1: Model description,
632 Geoscientific Model Development, 12, 4309–4346, 2019a.
633 Longo, M. et al.: The biophysics, ecology, and biogeochemistry of functionally diverse, vertically and horizontally
634 heterogeneous ecosystems: the Ecosystem Demography model, version 2.2 – part 2: Model evaluation for
635 tropical South America, Geoscientific Model Development, 12, 4347–4374, 2019b.
636 Lugo, A. E. and Rivera Batlle, C. T.: Leaf production, growth rate, and age of the palm Prestoea montana in the
637 Luquillo Experimental Forest, Puerto Rico, Journal of Tropical Ecology, 3, 151–161, 1987.
638 Lugo, A. E., Francis, J. K., and Frangi, J. L.: Prestoea montana (R. Graham) Nichols. Sierra palm. Palmaceae. Palm
639 family, Tech. Rep. SO-ITF-SM-82, US Department of Agriculture, Forest Service, International Institute of
640 Tropical Forestry, 1998.
641 Ma, R.-Y., Zhang, J.-L., Cavaleri, M. A., Sterck, F., Strijk, J. S., and Cao, K.-F.: Convergent evolution towards high
642 net carbon gain efficiency contributes to the shade tolerance of palms (Arecaceae), PLoS ONE, 10, e0140384.
643 2015.
644 Massoud, E. C. et al.: Identification of key parameters controlling demographically structured vegetation dynamics in
645 a land surface model: CLM4.5(FATES), Geoscientific Model Development, 12, 4133–4164, 2019.
646 Medvigy, D., Wofsy, S. C., Munger, J. W., Hollinger, D. Y., and Moorcroft, P. R.: Mechanistic scaling of ecosystem
647 function and dynamics in space and time: Ecosystem Demography model version 2, Journal of Geophysical
648 Research, 114, G01002, 2009.

https://doi.org/10.5194/gmd-2021-410
Preprint. Discussion started: 14 January 2022

649 Meunier, F. et al: Liana optical traits increase tropical forest albedo and reduce ecosystem productivity, Global Change
650 Biology, in revision.
651 Mirzaei, M., Huang, Y. F., El-Shafie, A., and Shatirah, A.: Application of the generalized likelihood uncertainty
652 estimation (GLUE) approach for assessing uncertainty in hydrological models: A review, Stochastic
653 Environmental Research and Risk Assessment, 29, 1265–1273, 2015.
654 Moorcroft, P. R., Hurtt, G. C., and Pacala, S. W.: A method for scaling vegetation dynamics: The ecosystem
655 demography model (ED), Ecological Monographs, 71, 557–586, 2001.
656 Muscarella, R. et al.: The global abundance of tree palms, Global Ecology and Biogeography, 29, 1495–1514, 2020.
657 Parker, G. et al.: Effects of hurricane disturbance on a tropical dry forest canopy in western Mexico, Forest Ecology
658 and management, 426, 39–52, 2018.
659 Paz, H. Vega-Ramos, F., and Arreola-Villa, F.: Understanding hurricane resistance and resilience in tropical dry forest
660 trees: A functional traits approach, Forest Ecology and Management, 426, 115-122, 2018.
661 Royo, A. A., Heartsill Scalley T., Moya, S., and Scatena, F. N.: Non-arborescent vegetation trajectories following
662 repeated hurricane disturbance: ephemeral versus enduring responses, Ecosphere, 27, 77, 2011.
663 Rutledge, B. T., Cannon, J. B., McIntyre, R. K., Holland, A. M., and Jack, S. B.: Tree, stand, and landscape factors
664 contributing to hurricane damage in a coastal plain forest: post-hurricane assessment in a longleaf pine
665 landscape, Forest Ecology and Management, 481, 118724, 2021.
666 Sakschewski, B. et al.: Resilience of Amazon forests emerges from plant trait diversity, Nature Climate Change, 6,
667 1032–1036, 2016.
668 Scatena, F. N., Silver, W., Siccama, T., Johnson, A., and Sanchez, M. J.: Biomass and nutrient content of the Bisley
669 Experimental Watersheds, Luquillo Experimental Forest, Puerto Rico, before and after hurricane Hugo,
670 1989, Biotropica, 25, 15–27, 1993.
671 Stein, M.: Large sample properties of simulations using Latin Hypercube sampling, Technometrics, 29, 143–151,
672 1987.
673 Taylor, J. A. and Lloyd, J.: Sources and Sinks of Atmospheric CO_2, Australian Journal of Botany, 40, 407–418, 1992.
674 Uriarte, M., Thompson, J., and Zimmerman, J. K.: Hurricane Maria tripled stem breaks and doubled tree mortality
675 relative to other major storms, Nature Communications, 10, 1362, 2019.
676 Walker, L. R.: Tree damage and recovery from hurricane Hugo in Luquillo Experimental Forest, Puerto Rico. Part A.
677 special issue: ecosystem, plant, and animal responses to hurricanes in the Caribbean, Biotropica, 23, 379–
678 385, 1991.
679 Wang, D., LeBauer, D. and Dietze, M.: Predicting yields of short-rotation hybrid poplar (Populus spp.) for the United
680 States through model-data synthesis, Ecological Applications, 23, 944–958, 2013.
681 Wang, G. and Eltahir, E. A. B.: Biosphere-atmosphere interactions over West Africa. II: Multiple climate equilibria,
682 Quarterly Journal of the Royal Meteorological Society, 126, 1261–1280, 2000.
683 Xiao, Z., Liang, S., Wang, J., Xiang, Y., Zhao X., and Song, J.: Long-time-series global land surface satellite leaf area
684 index product derived from MODIS and AVHRR surface reflectance, IEEE Transactions on Geoscience and
685 Remote Sensing, 54, 5301–5318, 2016.

https://doi.org/10.5194/gmd-2021-410
Preprint. Discussion started: 14 January 2022

Geoscientific Model Development Discussions

686 Xiao, Z., Liang, S., and Jiang, B.: Evaluation of four long time-series global leaf area index products, Agricultural and
687 Forest Meteorology, 246, 218–230, 2017.
688 Xu, X., Medvigy, D., Powers, J. S., Becknell, J. M., and Guan, K.: Diversity in plant hydraulic traits explains seasonal
689 and inter-annual variations of vegetation dynamics in seasonally dry tropical forests, New Phytologist, 212,
690 80–95, 2016.
691 Zanne, A. E. et al.: Data from: Towards a worldwide wood economics spectrum. Dryad Digital Repository.
692 https://doi.org/10.5061/dryad.234, 2009.
693 Zhang, J., Bras, R. L., and Heartsill Scalley, T.: Tree census at Bisley Experimental Watersheds three months after
694 hurricane Maria, Fort Collins, CO: Forest Service Research Data Archive, https://doi.org/10.2737/RDS-
695 2020-0012, 2020.
696 Zhang, J., Bras, R. L., and Heartsill Scalley, T.: Tree census at Bisley Experimental Watersheds between 1989 and
697 2014. In preparation.
698 Zhang, J., Heartsill Scalley, T., and Bras, R. L.: The importance of forest structure and composition on hurricane
699 effects. In revision.
700 Zhang, J., Heartsill Scalley, T., and Bras, R. L.: Parsing long-term tree recruitment, growth, and mortality to identify
701 hurricane Hugo's effects on the Luquillo Experimental Forest in Puerto Rico. In revision.
702 Zimmerman, J, K. et al.: Responses of tree species to hurricane winds in subtropical wet forest in Puerto Rico:
703 Implications for tropical tree life histories, Journal of Ecology, 82, 911–922, 1994.
704